ON THE AAR SUSCEPTIBILITY OF GRANITIC AND QUARTZITIC AGGREGATES IN VIEW OF PETROGRAPHIC CHARACTERISTICS AND ACCELERATED TESTING

Per Hagelia[1*], Isabel Fernandes[2*]

[1]Tunnel and Concrete Division, Norwegian Public Roads Adminsitration, Oslo, Norway

[2] Universidade do Porto, DGAOT/Centro de Geologia, Porto, Portugal

Abstract

Petrography is used as a first step in assessing the potential AAR-susceptibility of concrete aggregates. When an aggregate is classified as innocuous further testing is usually not mandatory. Thus, it is important to be aware of the complex petrographic characteristics of reactive aggregates, without which there is a risk that deleterious aggregates will be used with no special care. This paper reports on intriguing evidence from Norwegian and Portuguese field concretes and specimens from accelerated testing. ASR-gels formed in association with medium-grained granitic and quartzitic aggregates, characterised by strain free quartz and stable grain boundaries. ASR-gel formation sites preferably occurred in contact with micas and feldspars. Conversely, granitic mylonites characterised by annealed microcrystalline quartz and very low mica contents were mainly innocuous. The results suggest that quartz size in many cases is of subordinate importance, whilst the reactivity seems partly controlled by dissolution of feldspars and micas, perhaps also involving catalytic effects.

Keywords: *In situ* formed ASR-gel, granite, quartzite, quartz-size, mica, feldspar

1 INTRODUCTION

It is well established that alkali-silica reaction (ASR) takes place in concrete containing aggregates with microcrystalline quartz, cryptocrystalline silica or amorphous constituents such as glass. Thus, rocks such as mylonite, chert, sandstone, claystone and volcanites are susceptible to ASR [1,2]. Petrographic test methods for identification of reactive aggregates are, therefore, used in most countries around the world. When a concrete aggregate is regarded as innocuous on petrographic grounds then requirements for further testing by accelerated test methods are often not mandatory. For this reason it is very important to be aware of the full petrographic variety of potentially deleterious rock types.

Although research has continued over several decades, the ASR-susceptibility of certain rock aggregates still remains uncertain. Among these are the potential reactivity of relatively coarse grained (ca. 130 – 2000 μm) granitic rocks and quartzite. Such aggregates are considered to be innocuous in Norway [3], whilst further accelerated testing is required for Portuguese granites [4]. It is generally believed that the reactivity of aggregates is governed by the properties of silica, whilst much lesser attention has been given to the overall mineralogical composition. In early assessments regarding granitic rocks, straining effects in quartz such as the undulatory extinction were considered a good explanation for the performance of granitic aggregates, in some areas of the world [5,6]. However, soon the undulatory extinction was considered just a possible

* Correspondence to: per.hagelia@vegvesen.no and ifernand@fc.up.pt

indicator rather than a diagnostic feature of ASR-susceptibility [7-10], in part because it was applied out of context with the structural history of the rock. An important contribution was made by Wigum [11], who proposed the quantification of the average surface area of quartz through grain size measurement in fault rocks. It has also been verified that the recrystallization of the quartz can explain the decrease in the reactivity of strongly mylonitised rocks [12], since the evolution of smaller grains into larger ones with polygonisation of the boundaries leads to a smaller total quartz surface area [13,14]. Wenk et al. [15] demonstrated a positive correlation between ASR and quartz dislocation density. The authors found that the contribution of dislocations to the bulk energy increase of quartz is low, whilst dislocations provide favourable sites for dissolution and precipitation to occur. In addition, the comparison of two granitic aggregates from Spanish dams permitted to conclude that for granite the formation and storage of gel might be associated to microcracks rather than to subgrain boundaries [16].

The expansive ASR-gels always contain alkalis (Na & K), Si and Ca, and sometimes also Al, Mg, Fe and other elements (e.g. [17]). In summary, dissolution of silica is commonly regarded as the source of Si, whilst alkalis and Ca are supplied by the cement. However, feldspars also deliver alkalis [18,19], and even Si and Al to high alkaline solutions [20,21]. Experimental work also show that Si, Al and alkalis are leached from micas at high pH [20,22,23]. The objectives of this work were to:

- Document *in situ* formation of ASR-gel, being spatially in contact with coarse quartz, micas and feldspars.
- Discuss their origin, consequences and further research needs.

2 MATERIALS AND METHODS

2.1 Materials investigated

In the present work thin-sections of different samples of field concrete and test specimens were studied.

Bridge in Arendal, Norway. This arch bridge was opened for traffic in 1942. By mid-1970-ties the bridge deck was repaired due to cracking and crumbling of the concrete. One concrete core, V1 (Φ = 95 mm, 235 mm long), was extracted in 1977 from a mainly intact area of the bridge deck. The concrete aggregate consisted of amphibolite facies rocks from uncrushed fluvio-glacial material. The cement used was Norwegian Portland Cement, probably with about Na_2O_{eq} = 1.2 – 1.3 wt. %, which seems typical for old cements [24]. The water-cement (w/c) ratio was likely within the 0.5 to 0.6 interval.

Retaining wall in Oslo, Norway. The structure was cast in 1964 and had developed map cracking due to ASR. Norwegian Portland cement with about wt. 1.2 % Na_2O_{eq} was used with w/c-ratio of about 0.6. Abundant granitic gneiss had contributed to ASR here [25]. ASR-gel had formed in granitic aggregates with quartz sizes about 50-130 μm, but was not restricted to this range: Gels also occurred in grain sizes even exceeding 300 μm in concrete Core A (Φ = 100 mm, 260 mm long) [26], which was investigated further.

Wall belonging to an energy dissipation basin of a dam, Portugal. The wall was built in the 1972. The concrete was manufactured using a granitic rock from a quarry. There was no detailed information about the concrete composition. The top exposed surface of the wall shows map cracking with discoloration. A core (Φ = 90 mm, 400 mm long) was extracted in 2006 by drilling methods for petrographic examination of the concrete.

A concrete prism from laboratory tests of deformed granite was included in the study. The test was performed according to AAR-4.1 at 60ºC. The aggregate was crushed and sieved complying with the specifications in the standard. A cement type CEM I 42.5 R with 0.89% of Na_2O_{equiv}, an aggregate/cement (a/c) ratio of 0.25 and a water/cement (w/c) ratio of 0.45 was used [27]. The prisms expanded 0.070% in 20 weeks. Slices were cut with a diamond saw and thin-sections were prepared in order to verify the existence of manifestations of ASR such as cracks and alkali-silica gel.

Two series of mortar bars from AAR-2 [28] of a granitic mylonite tested in a previous study were included in this paper (samples 275 and 276 with thin-sections). This was due to their surprisingly low 14 days expansion results of 0.041 % and 0.075 % for samples 275 and 276, respectively, and with 0.119 %, and 0.150 % at 28 days. Although there is no field experience with this mylonite, the results suggest such mylonites should be innocuous or perhaps marginally reactive in field concrete [13, 29].

2.2 Methods for assessment and analysis

Optical microscopy

The study presented here was mainly based on petrographic examination. Conventional polished thin-sections of 30 μm thickness, measuring 25×45 mm, were prepared. Most thin-sections were produced by hand using several stages of grinding and lapping with powdered silicon carbide and final polishing with 0.25 μm diamond grit. The thin-sections of sample V1 were prepared automatically using a Thorlag machine. Water was used as a coolant at all stages.

The observation was performed with a Nikon Eclipse E400 POL optical microscope equipped with 10x ocular and objectives 5x, 10x and 20x. Microphotographs were obtained by AxioCam MRc and software AxioVision 3.1.

Scanning electron microscope and electron dispersive diffraction (SEM/EDS)

The thin-sections were sputtered with carbon in a JEOL JEE-4X Vacuum Evaporator and thus analysed in Scanning Electron Microscope JEOL JXA 8800M equipped with a EDS detector FEI QUANTA 400 FEG ESEM/EDAX PEGASUS X4M at CEMUP. Operating conditions were set at 15 kV and 20 nA, at high vacuum. The working distance was 10 mm, the collection time for the microanalyses of 50s with a dead time of approximately 30%. Standardless semi-quantitative analyses were obtained.

3 RESULTS

3.1 Norwegian bridge

Eight thin-sections from Core V1 were first examined in polarised light. The stone aggregate consisted of quartzite, granitic gneiss and much lesser amounts of amphibolite and metapelite. The quartzite contained muscovite and biotite and the granitic gneiss was mainly muscovite bearing with minor amounts of Fe-oxides. The quartz grain sizes of these main rock types varied between 500 and 2000 μm, being strain free or with a small degree of undulatory extinction. Such grains were commonly cracked/parted, forming about 50-300 μm sized segments with straight boundaries. Quartz contained frequent unidentified fluid inclusions, some of which formed discrete secondary trails. Micas were commonly 100-1000 μm in size. The sand fraction consisted mainly of quartz grains and some grains of feldspars, amphibole, biotite, granite and dolerite.

In situ formed pale to brown ASR-gels (10-400 μm) occurred scattered along the aggregate-cement paste interface in quartzite, most commonly in contact with muscovite and biotite grains (Figure 1). Locally apparent dissolution of quartz could be seen in association with micro cracks. No obvious dissolution could be observed along cracks/parting within single large quartz grains. Occasionally quartz dissolution phenomena were observed where fluid inclusion trails reached the surface of a quartzite aggregate.

One thin-section (V1-1) with ASR-gels was selected for SEM work, focusing on two micro domains. In one area (Figure 1, plane polarised light) a large brownish gel (400 μm x 100 μm) with paler gel rim had formed *in situ* in direct contact with muscovite (100 μm) and large quartz (1500 μm). The quartz grain was optically continuous, but was parted into < 100 to 300 μm sized fragments. The muscovite contained small amounts of Ca, Na, Mg and Fe, and there was no apparent compositional difference between undeformed and kinked muscovite, although the Al peak was lower relative to Si in the kink band. A gel layer in near

contact with muscovite (Z7) contained a little Al, whilst gel away (Z5) contained no Al. Otherwise all gels contained Si, Ca, K and Na (concentrations in descending order).

In the second micro domain dark brown gel with a pale rim had formed *in situ* in contact with biotite (75-250 μm) and large quartz (1000 μm) in the aggregate. The quartz with biotite grains in Figure 2 was optically continuous, yet parted into < 50 to 300 μm sized fragments.

3.2 Norwegian retaining wall

Eight thin-sections from Core A were examined in polarised light. The coarse aggregate consisted of granitic gneiss, impure limestone, some mylonite, sandstone/siltstone and claystone. The sand fraction consisted mainly of granitic gneiss, quartz, feldspar, mafic rocks and some silt and sandstone. In the coarse fraction granitic gneiss had reacted along with mainly mylonite. Typical reaction rims were observed around granitic gneiss in the core sample. ASR-gels reaching up to 250 x 1000 μm in size had formed at the interface with granitic aggregate in direct contact with K-feldspar (microcline) and quartz (Figure 3). Dark gels also occurred within aggregate in large albite grains. The quartz grain sizes with associated *in situ* formed gels were ranging in size from about 50 to 500 μm, being similar to feldspar sizes. The granitic gneiss also contained chlorite and biotite.

One thin-section (Per 1) was chosen for SEM, representing internal gels forming a network within quartz (sizes), albite, microcline and chlorite in a granitic aggregate. A feature of apparent feldspar dissolution was sometimes seen adjacent to gel. Dense gel within microcline had a little Al, probably reflecting the feldspar (Z4). Otherwise rosette-like gels occurred. In the case of analysis Z3 there was no Al. Both gels contained a little Na and K. It may further be noted that the gels in this sample appear to have more Si and lower Ca than the ones in Core V1. The relationship of ASR-gel depicted in Figure 3 seems to suggest that gels formed *in situ*. The right side image of Figure 3 indicates that gel swelling has taken place here, causing a local displacement along the quartz – microcline grain boundary.

3.3 Portuguese dam

Two polished thin-sections were examined in polarised light. The study of the aggregate particles showed medium grained two mica granite, mainly biotitic. There were no signs of deformation of the granitic aggregate. The quartz crystals showed straight boundaries, weak angles of undulatory extinction (mainly <15º) and variable sizes, more commonly around 1200 μm but some with 1800 μm. In the grains where parting occurs the sizes varied from about 100 μm to 800 μm. The boundaries were very often open and they were sometimes highlighted by iron oxides deposition. Cracks were observed crossing two particles of coarse aggregate and the cement paste. Alkali-silica gel was identified partially filling some of the cracks in the aggregate particles, mostly in the sectors closer to the cement paste, where the cracks showed wider openings. The gels were mostly brownish but not uniform in tonality, being lighter brown to colourless closer to the cement paste. The gels were compact, showing no crystalline structure. One location was selected for analysis by SEM/EDS.

One thin-section (CAA) was observed in order to confirm the presence of alkali-silica gel and to obtain its semi-quantitative composition. One micro domain was selected for analyses in which two branches of a crack cross a quartz grain of about 1200 μm and converged in a biotite crystal. The gel was denser in the stretches located closer to the interface with the cement paste. Five analyses were performed. The gel showed slightly variable composition with: high content of Si, lower Ca and K and, in some locations, very low contents of Na, Al and Mg. In Figure 4 a SEM image is presented and also the spectra obtained by EDS in two different spots along the crack. Both analyses are similar.

3.4 AAR-4 concrete prism made with Portuguese deformed granite

Four thin-sections were produced from one of the concrete prisms and analysed under polarised light. The aggregate was composed of deformed granite with inequigranular texture and preferential orientation of the minerals. Quartz crystals showed variable sizes from 100 to 200 μm but there were also crystals smaller than 50 μm. The quartz displayed irregular grain boundaries, undulatory extinction (~20º), deformation lamellae, and elongated, microcrystalline and sub-granulated crystals. Goticular forms of quartz were present in K-feldspars and plagioclases in myrmekite. Some bending of phyllosilicate cleavage plans and of twinning plans in plagioclases could be observed. Concerning the textural features this aggregate was classified as potentially reactive both by the petrography Portuguese standard and by AAR-1. Alkali-silica gel was identified in all the thin-sections. The gel occurred at the interfaces between the cement paste and the aggregate particles (Figure 5). In some sectors the gel was colourless, compact, with abundant cracks and in others it was brownish without a defined structure. One location was selected for SEM/EDS analysis.

One thin-section was selected for SEM/EDS study of the gel in a micro domain, where it occurs close to a large muscovite grain. A thin layer within the gel (between brown inner and outer pale gel) had an odd chemistry with vestigial Cl and S, probably due to contamination during thin-section preparation or from the glue. The gel showed layers of different tonality and different porosity, as shown by the higher content of C in Z2. Si was the main element, followed by Ca in variable content (Z3).

3.5 AAR-2 mortar bars made with Norwegian mylonite

Sample 275 [29] consisted mainly of completely annealed quartz ribbons in textural equilibrium with microcrystalline quartz (D_{50} = 55 μm) K-feldspar (orthoclase) and plagioclase (oligoclase). This sample contained only traces of biotite, Fe-Ti oxide and secondary chlorite, which in view of the expansion results cited above must be regarded as innocuous. ASR-gel formed after 14 days expansion, but in very insignificant quantities (Figure 6). However, sample 276 from a very similar mylonite (Quartz D_{50} = 43 μm) expanded just a bit more and had developed minor gel after 28 days of exposure [29]. Quartz grain sizes and textures were almost the same in both samples, whilst the main difference was somewhat higher biotite content in sample 276. The unusually low expansion of these mylonites has been attributed to the high temperature of formation (≥700 ºC), whilst the biotite content probably controlled the degree of reactivity (e.g. [13]).

4 DISCUSSION

The results presented above have proven that ASR-gel formation may take place also in quartz rich rocks with large quartz grains, ranging in size from ca 130 to 1000-2000 μm. These quartzes were strain free or with slightly undulatory extinction, with predominantly rational grain boundaries against other minerals. Yet, sheet silicates were in most cases present within the micro domains where ASR-gels had formed. Also feldspars appeared to have contributed to gel formation in several cases, as evidenced by their close association to gels as well as apparent dissolution phenomena. Similar reactivity was evident in accelerated testing according to AAR-4.1. Conversely, granitic mylonites with strain free annealed quartzes (D_{50} = 43-55 μm) were innocuous or very slowly reactive in AAR-2. The evidence clearly suggests that under certain circumstances the quartz grain size plays a subordinate role. Other mechanisms than quartz surface area seem required in order to supply Si to ASR gels. At high pH around 13-14, dissolution of mica and feldspar is in fact well established. Testing of rock-forming minerals according to ASTM Chemical Method C 289 (1 N NaOH at 80 ºC) have shown that biotite and quartz may release nearly identical concentrations of Si, being about twice that of the feldspars [20]). This result is in keeping with later research results. As regards feldspars it has been proven that alkalis as well as Si and Al are released in significant quantities into alkaline solution: Logarithms of dissolution rates for albite and K-feldspar are around -14 mol/cm²/sec at pH = 13-14 and

ambient T in water with low alkali contents (cf. [21] with references therein). In comparison, quartz dissolution rates at similar conditions are about -12 to -14 mol/cm^2/sec [30]. Dissolution rates of biotite and muscovite are also enhanced at very high pH. In particular element release is incongruous with early Si (and Al) release until stoichiometric dissolution commences at a more advanced stage [22,23]. These references also show that dissolution depends on the ions already in solution, and notably that dissolution of these silicates are much temperature dependent. Hence, a further understanding of accelerated test results versus evidence of ASR in field concrete should benefit much from further investigations into dissolution properties of aggregate minerals.

However, also catalytic effects of mica have also been invoked to explain locally enhanced silica dissolution and ASR-gel formation. Broekmans [31] argued on the basis of petrographic observation that sheet silicates are able to catalyse ASR. The mechanism is not precisely understood, although biotite is able to rise the local micro pH by about 0.6 units [32], which should indeed have an effect on silica dissolution in concrete. The possible impact of fluid inclusion-rich quartz on ASR-susceptibility has as yet not been investigated.

5 CONCLUSIONS

The present investigations, as based on petrographic examination and SEM of ASR-gel formation in granitic and quartzitic rocks have proven that:

- ASR-gel forms in relatively coarse grained and essentially strain free quartz.
- Quartz grain size is sometimes of subordinate importance in regard to ASR-susceptibility.
- Gel formation appears to be partly sustained by dissolution of feldspars and mica, with possible catalytic effects of sheet silicates.
- There is a need for further investigation of the role of feldspars and mica as regards ASR-susceptibility of concrete aggregates. Fluid inclusions should also be invoked, particularly in quartz.
- Investigation of results from accelerated test methods versus ASR in field concrete might take great advantage of a further understanding of mineral dissolution properties in high alkaline solutions similar to concrete pore solutions.

6 ACKNOWLEDGEMENTS

The authors gratefully acknowledge the assistance by Daniela Silva with SEM analysis. This work was developed under the scope of by GeoREMAT research Project and IMPROVE (Ref: PTDC/ECM/115486/2009) financed by FCT. PH also acknowledges the receipt of a travel grant from the Norwegian Public Roads Administration to Portugal in 2011.

7 REFERENCES

[1] Taylor, HFW (1997): Cement Chemistry (2nd Ed.) Thomas Telford Publishing.
[2] St. John, DA, Poole, AW, Sims, I (1998): Concrete Petrography – A handbook of Investigative Techniques, Arnold, London.
[3] Norwegian Concrete Association (2004): Alkali Aggregate Reactions in Concrete. Test Methods and Requirements to Test Laboratories, Publication No 3 (in Norwegian).
[4] Especificação LNEC E 461 (2007): Betões. Metodologias para prevenir reacções expansivas internas. Laboratório Nacional de Engenharia Civil, Lisboa: pp 6.
[5] Gogte, BS (1973): An evaluation of some common Indian rocks with special reference to alkali-aggregate reactions. Engineering Geology (7): 135-153.
[6] West, G (1994): Undulatory extinction of quartz in some British granites in relation to age and potential reactivity. Quarterly Journal of Engineering Geology (27/1): 69-74.

[7] Grattan-Bellew, PE (1992): Microcrystalline quartz, undulatory extinction & the alkali-silica reaction. In: Poole AB (editor). Proceedings of the 9th International Conference on Alkali-Aggregate Reaction in Concrete, London: 383-394.

[8] Kerrick, D, Hooton, R (1992): ASR of concrete aggregate quarried from a fault zone: results and petrographic interpretation of accelerated mortar bar tests. Cement and Concrete Research (22): 949-960.

[9] Shayan, A (1993): Alkali reactivity of deformed granitic rocks: a case study. Cement and Concrete Research (23): 1229-1236.

[10] RILEM TC 191-ARP: 'Alkali-reactivity and prevention-Assessment, specification and diagnosis of alkali -reactivity', RILEM Recommended Test Method AAR-1: Detection of potential alkali-reactivity of aggregates-Petrographic method, Materials and Structures, 36 (2003) 480-496.

[11] Wigum, BJ (1995): Examination of microstructural features of Norwegian cataclastic rocks and their use for predicting alkali-reactivity in concrete. Engineering Geology (40): 195-214.

[12] Locati, F, Marfil, S, Baldo, E (2010): Effect of ductile deformation of quartz-bearing rocks on the alkali-silica reaction. Engineering Geology (116), Issues (1-2): 117-128.

[13] Wigum, BJ, Hagelia, P, Haugen, M, Broekmans, MATM (2000): Alkali aggregate reactivity of Norwegian aggregates assessed by quantitative petrography. In: Bérubé, MA, Fournier, B and Durand, B (editors). Proceedings of the 11th International Conference on Alkali-Aggregate Reaction in Concrete, Québec: 533-542.

[14] Shayan, A, Xu, A, Morris, H (2008): Comparative study of the concrete prism test (CPT 60ºC, 100% RH) and other accelerated tests. Book of Abstracts and Proceedings (CD-Rom) of the 13th International Conference on Alkali-Aggregate Reaction in Concrete, Trondheim: pp 10.

[15] Wenk, H-R, Monteiro, PJM, Shomglin, K (2008): Relationship between aggregate microstructure and mortar expansion. A case study of deformed granitic rocks from Santa Rosa mylonite zone. Journal of Materials and Science (43): 1278-1285.

[16] Velasco-Torres, A, Aejos, P, Soriano, J (2010): Comparative study of the alkali-silica reaction (ASR) in granitic aggregates. Estudios Geológicos (66), Issue (1): 105-114.

[17] Knudsen, T, Thaulow, N (1975): Quantitative microanalysis of alkali-silicagel in concrete. Cement and Concrete Research (5): 443-454.

[18] Constantiner, D, Diamond, S (2003): Alkali release from feldspars into pore solutions. Cement and Concrete Research (33): 549-554.

[19] Bérubé, M-A and Fournier, B (2004): Alkali releasable by aggregate in concrete – Significance and test methods. In: Tang, M, Deng, M (editors). Proceedings of the 12th International Conference on Alkali-Aggregate Reactions in Concrete, Beijing, China, Vol. I, 17-30.

[20] Choquette, M, Bérubé, M-A, Locat, J (1991): Behavior of common rock-forming minerals in a strongly basic NaOH solution. Canadian Mineralogist (29): 163-173.

[21] Locati, F, Marfil, S, Baldo, E, Maize, P (2010): Na_2O, K_2O, SiO_2 and Al_2O_3 release from potassic and calcic-sodic feldspars into alkaline solutions. Cement and Concrete Research (40): 1189-1196.

[22] Malmstrøm, M, Banwart, S (1997): Biotite dissolution at 25 oC: The pH dependence of dissolution rate and stoichiometry. Geochimica et Cosmochimica Acta (61): 2779-2799.

[23] Oelkers, EH, Schott, J, Gauthier, J-M, Herrero-Roncal, T (2008): An experimental study of the dissolution mechanism and rates of muscovite. Geochimica et Cosmochimica Acta (72): 4948-4961.

[24] Jensen, V (1993): Alkali Aggregate Reactions in Southern Norway. Dr. Technicae thesis, NTH University of Trondheim.

[25] Jensen, V, Haugen, M (1996): Cracking in the Oslo region – Investigations of possible alkali aggregate reactions in 8 concrete structures by structural analysis. SINTEF report 700461.40 (in Norwegian).

[26] Hagelia, P (2004): Origin of map cracking in view of the distribution of air voids, -strength and ASR-gel. In: Tang, M, Deng, M (editors). Proceedings of the 12th International Conference on Alkali-Aggregate Reactions in Concrete, Beijing, China, Vol. II, 870-881.

[27] RILEM AAR-4.1 (2006): Detection of potential alkali-reactivity of aggregates – 60º C accelerated method for aggregate combinations using concrete prisms. Committee Document RILEM/TC-ACS/11/06.

[28] RILEM TC 106-AAR (2000):Alkali Aggregate Reaction' A. TC 106-2- Detection of Potential Alkali-Reactivity of Aggregates –The Ultra-Accelerated Mortar-Bar Test B. TC 106-3-Detection of Potential

Alkali-Reactivity of Aggregates-Method for Aggregate Combinations Using Concrete Prisms, Materials and Structures, 33 283-293.
[29] Hagelia, P (1999): Comparison of three test methods for alkali reactivity. Technology Department, Norwegian Public Roads Administration, Internal report No. 2076 (in Norwegian).
[30] Dove, PM, Rimstidt, JD (1994): Silica – water interaction. In: Heaney, PJ, Prewitt, CT, Gibbs, GV (editors): Silica. Reviews in Mineralogy (29): 259-308.
[31] Broekmans, MATM (2002): The alkali-silica reaction: mineralogical and geochemical aspects of some Dutch concretes and Norwegian mylonites. PhD-thesis Utrecht University, The Netherlands. Geologica Ultraiectina (217): pp 144.
[32] Boles, JR, Johnson, KS (1984): Influence of mica surfaces on pore-water pH. Chemical Geology, 32, 303-317.

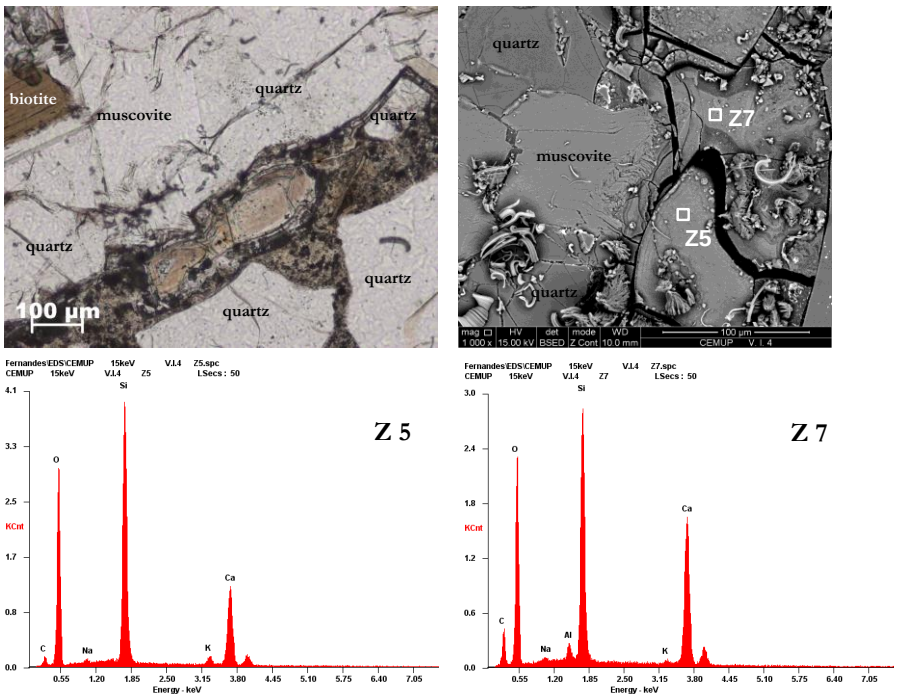

FIGURE 1: ASR-gel (Z5, Z7) formed *in situ* in contact with muscovite and medium grained quartz (1500 µm). Plane polarised light and SEM backscatter. The curved and branched deposits represent calcium carbonate which had grown from gel (old thin section). Core V-1.

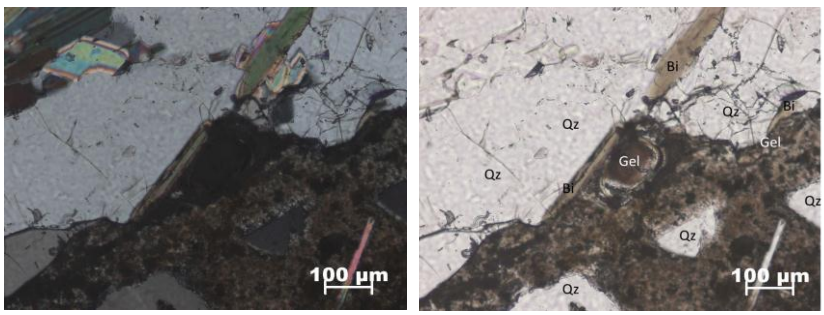

FIGURE 2: Brown ASR-gels formed *in situ*, typically coinciding with presence of biotite. The adjacent quartz (ca. 1000 µm) was strain free and in optical continuum, exhibited parting. Left: cross polarised light, right: plane polarised light. Sample V1.

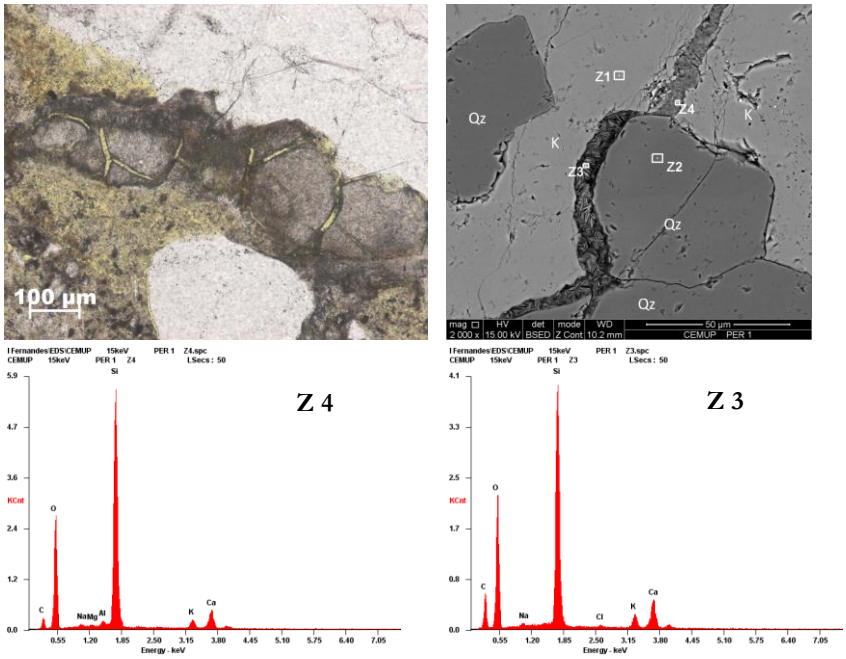

FIGURE 3: Upper image: Brownish ASR-gels formed *in situ* on medium grained granitic gneiss (plane polarised light) and within granitic gneiss (SEM backscatter). Rosette-like gel (Z3) and dense gel (Z4) on grain boundaries with quartz and microcline (K). Notice the apparent dissolution of feldspar near Al bearing Z4. Core A- Per 1.

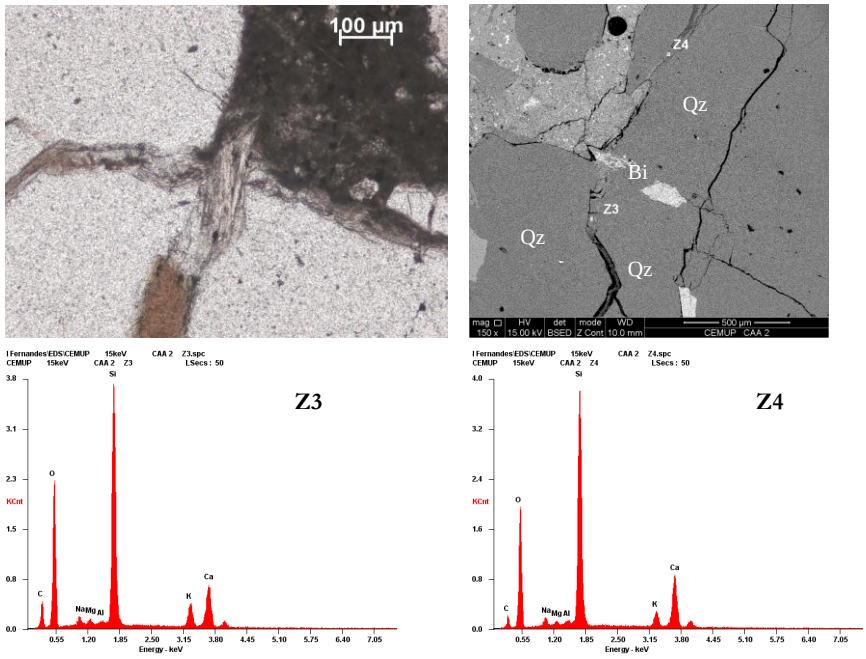

FIGURE 4: ASR-gel occurring within coarse quartz (Qz) with micro cracks converging to a biotite crystal (Bi). Plane polarised light and backscatter image. Analysed gels (Z3 and Z4) refer to the EDS spectra below. Concrete from the wall of an energy dissipation basin (CAA).

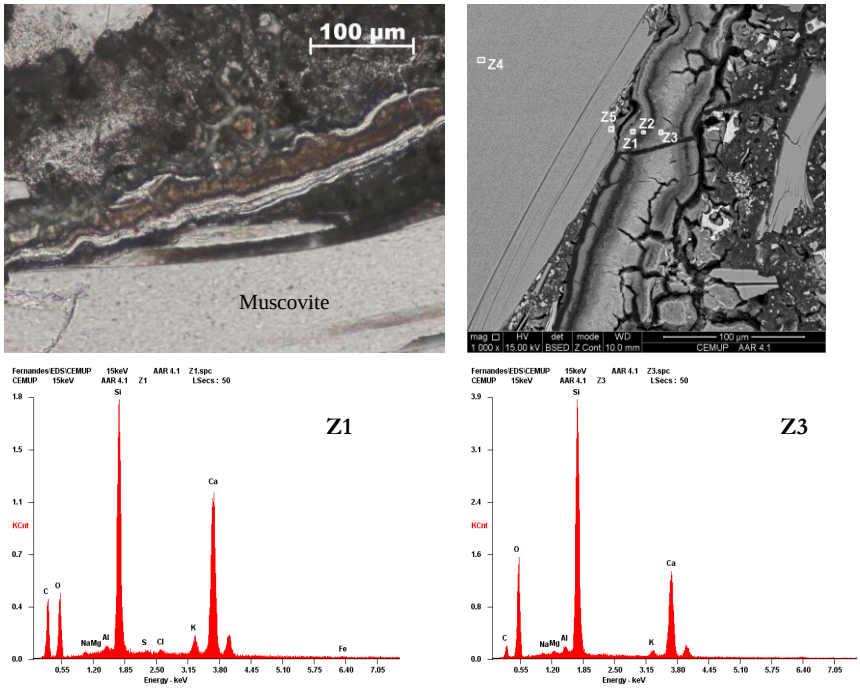

FIGURE 5: Upper left: ASR-gel in the interface with the cement paste close to a muscovite crystal (plane polarised light). Upper right: Backscatter image showing ASR gel with a zoned structure. Analysed gels (Z1 and Z3) refer to the EDS spectra below. Sample AAR-4.

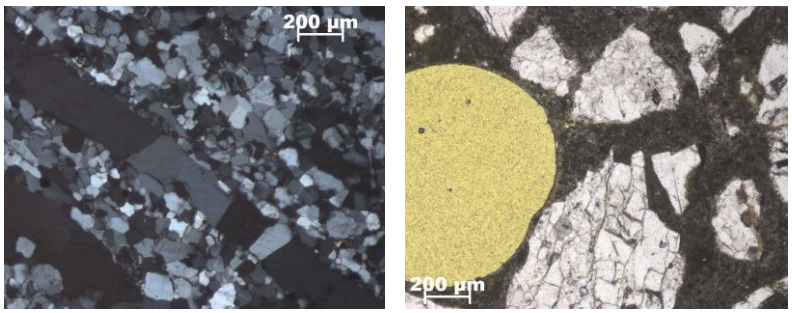

FIGURE 6: Innocuous Norwegian mylonite, sample 275. Left image (crossed polarised light) shows the annealed texture, with much quartz < 100 µm. Right image (plane polarised light) shows lack of ASR-gel formation after 14 days exposure according to AAR-2. Notice the typical scarcity of mica and accentuated grain boundaries.